Sustainable Processes Connect
2026, Vol. 2, Cite as: doi:10.x/journal.x.x.x

SCIFINITI PUBLISHING

OPEN ACCESS

Research Article

Green Sustainable Synthesis of Silver Nanoparticles from Extracts of Garden Spearmint *Mentha spicata* for Antibiotic and Antioxidant Activities

Seyedali Mousavi[1], Payam Ashooriyan[1], Mehrasa Yazdanpanah Rostami[1], Mahsa Erfani[1], Poonam Singh Nigam[*2]

1. Department of Biotechnology, Faculty of Chemical Engineering, Babol Noshirvani University of Technology, Babol, Iran
2. Biomedical Sciences Research Institute, Faculty of Life and Health Sciences, Ulster University, Coleraine, N. Ireland, UK

***Corresponding Author: p.singh@ulster.ac.uk** https://orcid.org/0000-0001-8505-5382

Authors	Email	ORCID
Seyedali Mousavi	seyedali.mousavi716@gmail.com	https://orcid.org/0009-0005-4704-8102
Payam Ashooriyan	P.ashooriyan@gmail.com	https://orcid.org/0000-0002-0107-8091
Mehrasa Yazdanpanah Rostami	Mehrasa.yazdanpanah.rostami@gmail.com	https://orcid.org/0009-0001-5024-4404
Mahsa Erfani	Mahsaerfani697@gmail.com	https://orcid.org/0009-0003-0622-2296
Poonam Singh Nigam	p.singh@ulster.ac.uk	https://orcid.org/0000-0001-8505-5382

Abstract

Silver nanoparticles (AgNPs) were synthesized using a green route with *Mentha spicata* (*M. spicata*) extract. The extract was prepared through three methods (Soxhlet, maceration, and ultrasonic-assisted extraction) and the yields were compared as weight percentages of dry plant material. Soxhlet extraction gave the highest yield of 34.36% while ultrasonic-assisted extraction and maceration provided yields of 18.21% and 11.80%, respectively. Although ultrasonic-assisted extraction method had lower yield, it was selected as an optimal one due to shorter extraction time, less solvent consumption, and high energy efficiency among other methods. The antioxidant capacity of *M. spicata* extract was very high with total polyphenol content at 106.22 mg gallic acid equivalents per gram of dry plant material and IC_{50} at 34.02 µg/mL in the DPPH assay; key synthesis parameters for AgNPs were optimized pH (9), temperature (60 °C), and extract concentration (1.0 g/L). Characterization by X-ray diffraction, Fourier-transform infrared spectroscopy, and scanning electron microscopy confirmed the crystalline structure, functional groups, and average particle size of about 58.41 nm; these synthesized AgNPs showed significant antibacterial activity against

Staphylococcus aureus, *Proteus mirabilis*, and *Salmonella typhimurium* at a concentration of 5 mg/mL to emphasize optimizing extraction and synthesis conditions for better bioactivity of nanoparticles.

Keywords: green synthesis; extraction techniques, *Mentha spicata,* silver nanoparticles, antibacterial activity, antioxidant activity

1. Introduction

In recent years, metal nanoparticles have attracted the attention of researchers due to their physicochemical, antibacterial properties and wide applications [1]. Although traditional nanoparticle synthesis methods are effective, they often involve hazardous chemicals and are energy-intensive. These syntheses also produce toxic by-products, which raise concerns about environmental safety and human health [2].

In order to mitigate these problems, environmentally friendly methods have been developed as practical and nature-friendly solutions [2,3]. These methods use biological agents such as plant extracts, microorganisms and biomolecules to convert metal ions into nanoparticles under mild conditions [4]. Green synthesis of nanoparticles provides several advantages compared to traditional chemical methods, such as reduced toxicity, cost savings, simplicity and improved biocompatibility of the produced nanoparticles [5]. The synthesis of nanoparticles using extracts of herbs is beneficial due to the abundance of natural bioactive compounds, such as polyphenols, flavonoids and other photochemical compounds, which have been reported in edible culinary herbs contributing to antiproliferative, antioxidant and antibacterial activities [6].

Mentha is a widespread aromatic plant with a rich phytochemical composition. Its four different species have shown significant potential for their applications due to their antimicrobial and cytotoxic activities [7]. The high content of polyphenols and other bioactive compounds in these materials not only enables efficient formation of nanoparticles but also confers significant antioxidant and antimicrobial properties to the produced AgNPs. In previous studies, the synthesis of AgNPs using *M. spicata* extracts has been investigated and has shown promising biological activities [8]. However, systematic comparison of extraction methods and optimization of AgNP synthesis parameters is still limited. In this study, we have performed an in-depth analysis of the green synthesis of AgNPs using *M. spicata* extracts. Different extraction methods, including ultrasonic extraction, Soxhlet extraction, and maceration, were investigated and key synthesis parameters, including pH, temperature, reaction time, and extract concentration, were systematically optimised to increase the yield of nanoparticles and their biological activity. The synthesised nanoparticles were comprehensively characterised. In contrast to previous studies, this work not only systematically compares multiple extraction methods but also optimizes key synthesis parameters to enhance nanoparticle yield, size uniformity, and biological activity, providing new insights into the green synthesis of *M. spicata*-mediated AgNPs.

This study aimed to conduct a comprehensive analysis of the effect of extraction methods and synthesis conditions on the properties and biological activities of AgNPs synthesised with *M. spicata* extracts, optimising a sustainable green sustainable synthesis process of silver nanoparticles.

2. Materials and Methods

Fresh *M. spicata* leaves were collected from the local area, and various extraction methods, including Soxhlet, ultrasonic, and maceration, were used to create the extracts. Unless otherwise noted, Merck (Darmstadt, Germany) provided silver nitrate ($AgNO_3$, ≥99.9 %), ethanol (80 %, v/v), methanol, Folin–Ciocalteu reagent, gallic acid, ascorbic acid, sodium carbonate, 2,2-diphenyl-1-picrylhydrazyl (DPPH), sulfuric acid, and calcium chloride dihydrate. Additionally, Merck provided the antibiotics gentamicin, ciprofloxacin, and sulfamethoxazole-trimethoprim. The American Type Culture Collection (ATCC) provided the bacterial strains used in this study, which were *S.typhimurium* (ATCC 14028), *Staphylococcus aureus* (ATCC 29213), and *Proteus mirabilis* (ATCC 12453). Every chemical and reagent used was analytical grade and did not require any additional purification.

2.1 Preparation of the *M. spicata* Extract

M. spicata leaves were gathered from the outskirts of Rostam-Kola in the Iranian province of Mazandaran. The fresh leaves were separated from the stems and other plant parts after being cleaned of dust and impurities using distilled water. To eliminate all moisture, the leaves were air-dried for approximately a month at room temperature in a well-ventilated, shaded area. Following complete drying, the leaves were ground into a fine powder using a mechanical grinder and kept dry in airtight containers until needed [9].

2.2. Extraction Methods

2.2.1. Soxhlet Extraction

A closed-end filter paper containing fifteen grams of dried powdered *M. spicata* leaves was put inside the Soxhlet apparatus. Extraction was performed using 300 mL of 80% ethanol for 24 hours under reflux conditions [10]. The extract was subsequently filtered and kept at 4°C until it was needed for further use.

2.2.2. Maceration

A total of 1.5 grams of dried powdered plant material was combined with 30 mL of 80% ethanol, sealed tightly, and continuously stirred at 10 rpm for 24 hours at room temperature, with manual shaking every 4 hours [11]. After filtration, the extract was collected from the mixture.

2.2.3. Ultrasonication

A 0.5 gram amount of dried powdered plant material was combined with 10 mL of ethanol (at concentrations of 60%, 80%, or 96%) and sonicated using a 7 mm ultrasonic probe at 70% power for durations of 4, 5, or 6 minutes [9]. After that, the extracts were filtered and stored in airtight containers for later use.

2.3. Biosynthesis of Silver Nanoparticles (AgNPs)

For the biological synthesis of silver nanoparticles, 1.5 g of dried *M. spicata* leaf powder underwent ultrasonic extraction using 80% ethanol. The extract was filtered through Whatman filter paper to remove solid residues and then oven-dried at 35 °C for 24 hours. The dried ethanolic extract was subsequently redissolved in distilled water to a final concentration of 1 g/L, and the pH of this aqueous solution was adjusted to 9 using a calibrated pH meter, as these conditions critically influence nanoparticle formation, size, and stability [12]. A 1 mM $AgNO_3$ solution was added dropwise to the aqueous extract under continuous stirring at 60 °C, and the reaction progress was monitored by

measuring UV–Vis absorbance at 420 nm at multiple time points. After the reaction reached completion, indicated by maximum absorbance and color change, the mixture was centrifuged at 10,000 rpm for 15 minutes, washed three times with deionized water to remove residual ions and solvents, and oven-dried at 70 °C for 24 hours. The effects of extract concentration, pH, temperature, and reaction time on nanoparticle synthesis were systematically evaluated to optimize the formation and stability of AgNPs.

2.4. Effect of Extract Concentration on Nanoparticle Synthesis

The effect of extract concentration on AgNP synthesis was investigated using aqueous solutions of the dried ethanolic extract at concentrations of 0.1, 0.25, 0.5, and 1 g/L [13]. 20 mL of the extract and 50 mL of a 1 mM silver nitrate solution were mixed for each concentration. For each concentration, 20 mL of the extract solution was mixed with 50 mL of 1 mM $AgNO_3$ under constant stirring at 65 °C. No additional $AgNO_3$ was added; the dropwise addition mentioned previously refers to gradual mixing to ensure uniform reaction. Using a spectrophotometer, absorbance at 420 nm was measured at 15, 30, 60, and 1440 minutes [13].

2.5. Effect of Temperature

The effect of temperature on AgNP synthesis was investigated at room temperature, 50, 60, and 70 °C using the aqueous solution of the dried extract (1 g/L) at the optimized pH 9. At 420 nm, absorbance was measured. Temperature has a major impact on nucleation and growth rates; higher temperatures speed up the reduction of silver ions but may also result in larger particle sizes due to aggregation. Therefore, accurate temperature control is essential for the desired properties of nanoparticles [9].

2.6. Effect of pH

The optimized concentration of dried ethanolic extract (1 g/L) was dissolved in distilled water, and the pH of the solution was adjusted to 6, 7, 8, and 9 using a calibrated pH meter. A 1 mM $AgNO_3$ solution was then added to the aqueous extract solution, and the reaction was carried out at 60 °C under magnetic stirring. The absorbance of the samples was measured at a wavelength of 420 nm. To move on to the following phases of the experiments, the one with the highest absorbance value was chosen [14].

2.7. Influence of Reaction Duration

A 1 g/L optimized extract concentration and a 1 mM silver nitrate solution were made in order to examine the reaction time [13, 15], with the pH of the distilled water set to 9. Silver nanoparticle formation was noted while the mixture was kept at 60 °C with constant stirring. At intervals of 15, 30, 60, and 1440 minutes, absorbance measurements at 420 nm were obtained to evaluate the progress of nanoparticle synthesis.

2.8. Collection and Purification of AgNPs

The reaction mixture showing the highest absorbance under the optimized conditions (extract concentration, pH, and temperature) was collected for nanoparticle purification. The AgNPs were centrifuged at 10,000 rpm for 15 minutes, and the resulting precipitate was washed three times with deionized water to remove any residual ethanol or unreacted silver ions. The purified nanoparticles were then oven-dried at 70 °C for 24 hours and stored for subsequent characterization using SEM, XRD, and FTIR. This procedure ensured complete removal of solvents and reactants, providing reproducible samples for physicochemical and biological analyses.

2.9. Characterization of Silver Nanoparticles

2.9.1. UV-Visible Spectroscopy

UV–Vis spectroscopy was performed using a Shimadzu spectrophotometer over the wavelength range of 220–620 nm to examine the optical behavior of the synthesized AgNPs. The formation of nanoparticles was confirmed by the presence of a characteristic surface plasmon resonance (SPR) peak. Absorbance values were recorded directly without normalization [16, 17].

2.9.2. Functional Group Identification

The functional groups in the *M. spicata* extract that aid in the reduction and stabilization of silver ions were identified through Fourier Transform Infrared (FTIR) spectroscopy analysis [18].

2.9.3. X-Ray Diffraction (XRD)

The crystalline structure and phase purity of the produced AgNPs were examined using X-Ray Diffraction (XRD) analysis using Cu Kα radiation, confirming their face-centered cubic crystal phase characteristic [19].

2.9.4. Morphological Analysis

The size and form of the produced AgNPs were examined using scanning electron microscopy (SEM) analysis. This technique uses electron beams to create intricate three-dimensional images [20].

2.9.5. Anti-oxidant activity

The Folin–Ciocalteu colorimetric method was used to determine the total phenolic content (TPC) of *M. spicata* leaves [21]. Whatman No. was used to filter the mixture. Before being used in further biochemical analyses, the filtrate was oven-dried at 35°C for 24 hours using one filter paper. A 1000 ppm stock solution of gallic acid was made in 70% methanol, and standard solutions of 12.5, 25, 50, and 100 ppm were acquired in order to create a calibration curve. 0.5 mL of the solution and 2.5 mL of 0.5 M Folin-Ciocalteu reagent were mixed for both standards and samples. Two milliliters of 7.5 percent sodium carbonate were added after five minutes. After 30 minutes of dark room temperature incubation, the mixture's absorbance at 720 nm was measured. A gallic acid calibration curve was used to calculate total phenolic content (TPC), which was then expressed as mg GAE per gram of dry extract [21].

2.10. Antibacterial Activity of Synthesized Nanoparticles

2.10.1. Disc Diffusion Method

Following the procedure described by Kirby-Bauer in 2009 [22], the antibacterial efficacy of *M. spicata* extracts and biosynthesized AgNPs was evaluated using the disc diffusion technique, with pH adjusted to 7.2–7.4. pH 7.2–7.4 was adjusted. Three common bacterial strains were tested: *S. typhimurium* (ATCC 14028), *Proteus mirabilis* (ATCC 12453), and *Staphylococcus aureus* (ATCC 29213). Sterile saline was used to adjust bacterial suspensions made from 24-hour cultures on blood agar to the 0.5 McFarland standard. Using sterile forceps, sterile discs containing 20 µL of either AgNPs (0.1–5 mg/mL) or plant extract (2.5–25 mg/mL) were carefully placed on the agar surface. Antibiotic discs containing gentamicin, ciprofloxacin, and sulfamethoxazole-trimethoprim were placed on the plates as positive controls. For a full day, the plates were incubated at 37 °C. The inhibition zones were measured to evaluate after incubation.

2.10.2. Tube dilution screening (qualitative)

A preliminary tube-dilution screening was performed to identify the effective concentration range of biosynthesized AgNPs for subsequent disc diffusion testing. Serial two-fold dilutions of AgNP suspensions (0.1–5 mg/mL) were prepared in nutrient broth and incubated with test organisms. This assay was used only as a qualitative screening to select concentrations for disc diffusion assays; formal MIC and MBC determinations were not conducted in the present study.

3. Results and discussion

3.1. The extraction efficiency of *M. spicata* plants

Three methods were used to assess *M. spicata* leaf extraction efficiency. Soxhlet extraction, maceration, and ultrasonic-assisted extraction were some of these methods. Soxhlet extraction was the most effective of the traditional techniques, producing 0.3436 g of extract per gram of dry plant material after 24 hours. On the other hand, under the same circumstances, maceration demonstrated a much lower extraction efficiency of 0.1180. Different combinations of extraction times (4, 5, and 6 minutes) and ethanol concentrations (60%, 80%, and 96%) were tested in order to optimize the ultrasonic extraction process. Table 1 provides a comparative overview of the different extraction methods employed in this study. the extraction efficiency of *M. spicata* plants by ultrasonic method is presented in Table 2. Eighty percent ethanol and six minutes of sonication produced the highest extraction yield. This was determined to be the ideal setting for further research. Although ultrasonic-assisted extraction provided slightly lower yield compared to Soxhlet extraction, it was selected as the optimal method due to its significantly lower energy consumption, reduced solvent use, shorter extraction time, and overall sustainability advantages.

Table 1. A comparative summary of the extraction methods and their effects on AgNP synthesis

Extraction method	Extraction time	Solvent consumption	Relative extract yield	AgNP formation efficiency
Soxhlet extraction	Long	High	High	Moderate
Maceration	Very long	Moderate	Moderate	Low-moderate
Ultrasonic-assisted extraction	Short	Low	High	High

Table 2: Extraction efficiency of *M. spicata* plants by ultrasonic method

Method	Dry weight of the plant (g)	Time (min)	Ethanol (%)	Weight efficiency (%, w/w, based on dry plant mass)
Ultrasonic method	0.5	4	60	2.1673 ± 0.2 ^{h}
			80	4.7766 ± 0.3 ^{g}
			90	0.9759 ± 0.06 ^{i}
	0.5	5	60	16.9298 ± 0.3 ^{c}
			80	17.2846 ± 0.2 ^{b}
			96	9.5371 ± 0.4 ^{f}
	0.5	6	60	12.0775 ± 0.3 ^{d}
			80	18.2090 ± 0.5 ^{a}
			96	10.8270 ± 0.4 ^{e}

Results are expressed as mean ± standard deviation (SD) (n = 3). Statistical analysis was performed using one-way analysis of variance (ANOVA) followed by Tukey's post hoc test in SPSS software. Differences were considered statistically significant at $p < 0.05$. Mean values in the same column with different superscript letters (a–i) indicate significant differences.

3.2. The green synthesis of silver nanoparticles

3.2.1 The effect of the concentration

The concentration of *M. spicata* extract had a significant impact on the generation of AgNPs [23]. A quick and striking change in color, from light brown to a deep brown shade in just one hour, demonstrated that increasing the extract amount accelerated the reaction [23, 24]. Due to the surface plasmon resonance phenomenon, this obvious color change usually indicates the formation of AgNPs [17].

As shown in **Fig. 1**. Greater production of nanoparticles was confirmed by increased absorbance at 420 nm at higher extract concentrations. At all-time points (15, 30, 60, and 1440 min), the 1 g/L concentration displayed the highest absorbance values, suggesting the quickest and most effective synthesis [25]. Lower concentrations (0.1, 0.25, and 0.5 g/L), on the other hand, displayed slower reaction rates, lower yields, less noticeable color changes, and lower absorbance values [26].

Increased extract concentrations result in improved synthesis, which is attributed to the increased availability of phytochemicals such as polyphenols and flavonoids. According to Vanlalveni et al., these bioactive constituents act as natural agents responsible for both stabilization and reduction during the synthesis process [12]. The results align with

Ghosh et al study [27], which demonstrated that increasing plant extract concentration accelerates silver ion reduction, leading to enhanced nanoparticle production and better control over particle size. Thus, the ideal extract concentration for further experimental procedures was chosen to be 1 g/L.

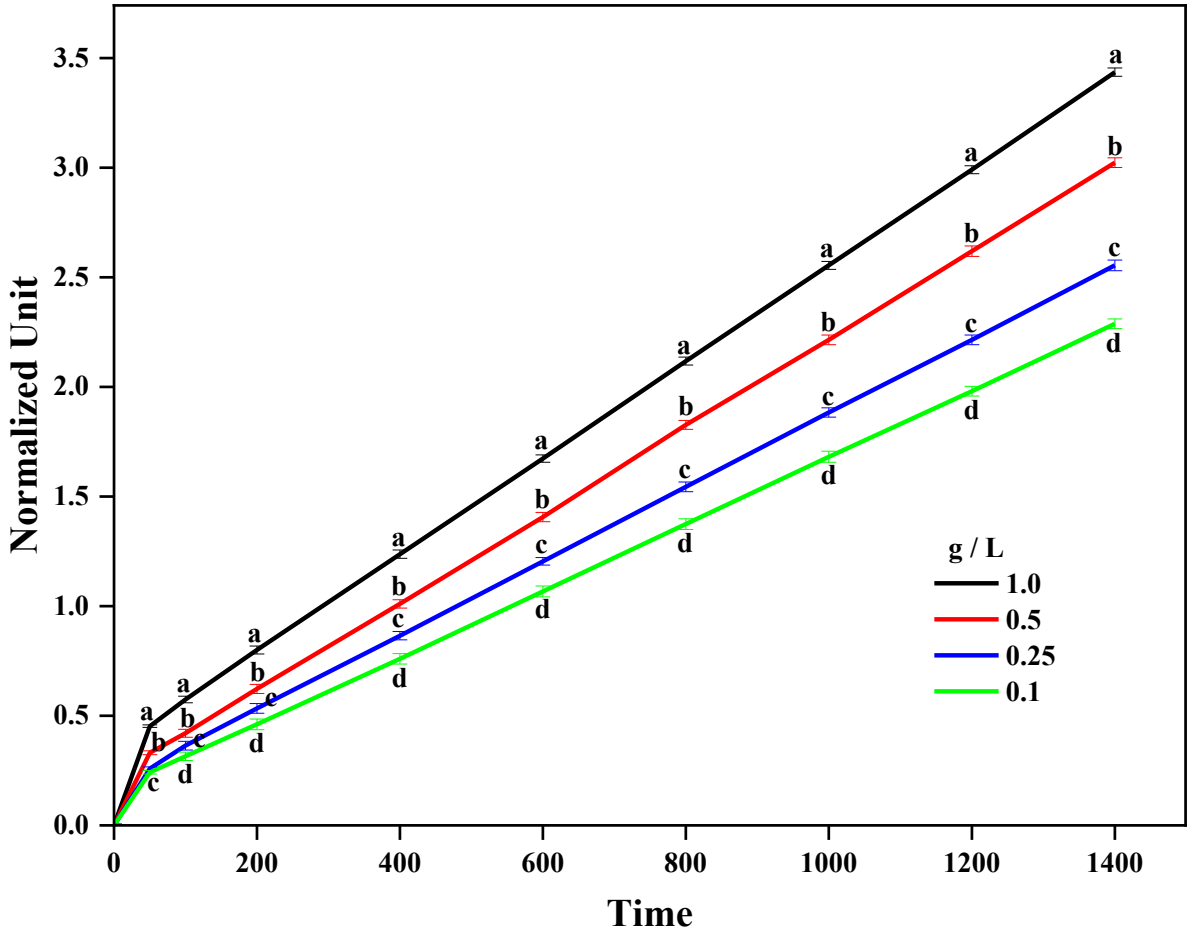

Fig. 1 Effect of extract concentration on AgNPs synthesis at different time points. Data are shown as mean ± SD (n = 3). Different superscript letters (a–d) indicate statistically significant differences at each time point, determined by one-way ANOVA followed by Tukey's test using SPSS ($p < 0.05$).

3.2.2. The effect of pH

The production of AgNPs was significantly impacted by the pH of the reaction mixture. Alkaline environments promote the reduction of silver ions, as evidenced by the rate of AgNP formation increasing as pH levels rose [28]. By increasing the ionization of the phytochemicals in the extract, particularly phenolic compounds, which increases their reducing potential, elevated pH levels speed up the creation of nanoparticles [29]. The fastest and most efficient synthesis occurred at pH 9 with an extract concentration of 1 g/L and a reaction temperature of 60 °C. Since this pH was determined to be the optimal value for the formation of nanoparticles, it was selected for further research. A **Fig.**

2 shows the reaction mixture's visual color changes and corresponding UV-Vis absorbance spectra at various pH levels to confirm increased nanoparticle formation at alkaline pH.

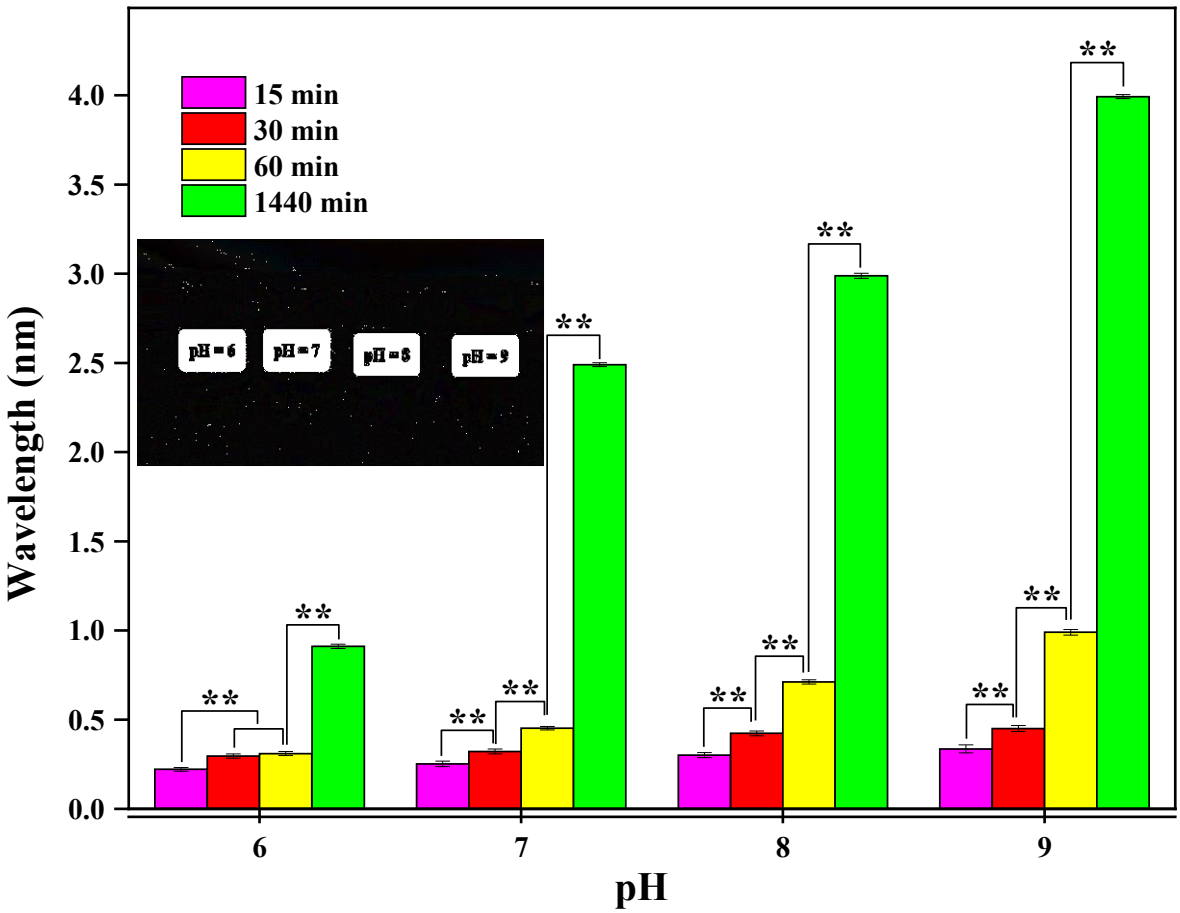

Fig. 2 Effect of pH on the synthesis of AgNPs. The graph shows the variation in nanoparticle formation at different pH values. indicates statistically significant differences between groups ($P < 0.05$).

3.2.3. The effect of temperature

The rate and effectiveness of the synthesis of AgNPs were significantly impacted by temperature [30]. Incr Raising the temperature shortened the time it took for nanoparticle formation by speeding up the reduction of silver ions [31,32]. The increased molecular kinetics and reactivity at higher temperatures are consistent with this inverse relationship between temperature and synthesis time [32]. AgNP formation was observed at 25 °C, 50 °C, 60 °C, and 70 °C at a fixed extract concentration of 1 g/L. As shown in **Fig. 3**. At 25°C, the reaction took roughly 10 hours; at 50°C and 60°C, the times dropped to 5 hours and 30 minutes, respectively. Nanoparticle agglomeration resulted from extended exposure, despite a slight increase in reaction rate at 70°C. Thus, the ideal temperature for creating consistent and stable nanoparticles was found to be 60°C.

Within 30 minutes, silver nanoparticle nucleation and growth were seen, with the first changes becoming apparent as early as 10 minutes. According to these results, higher temperatures speed up the formation of nanoparticles while preserving stability in ideal circumstances [33].

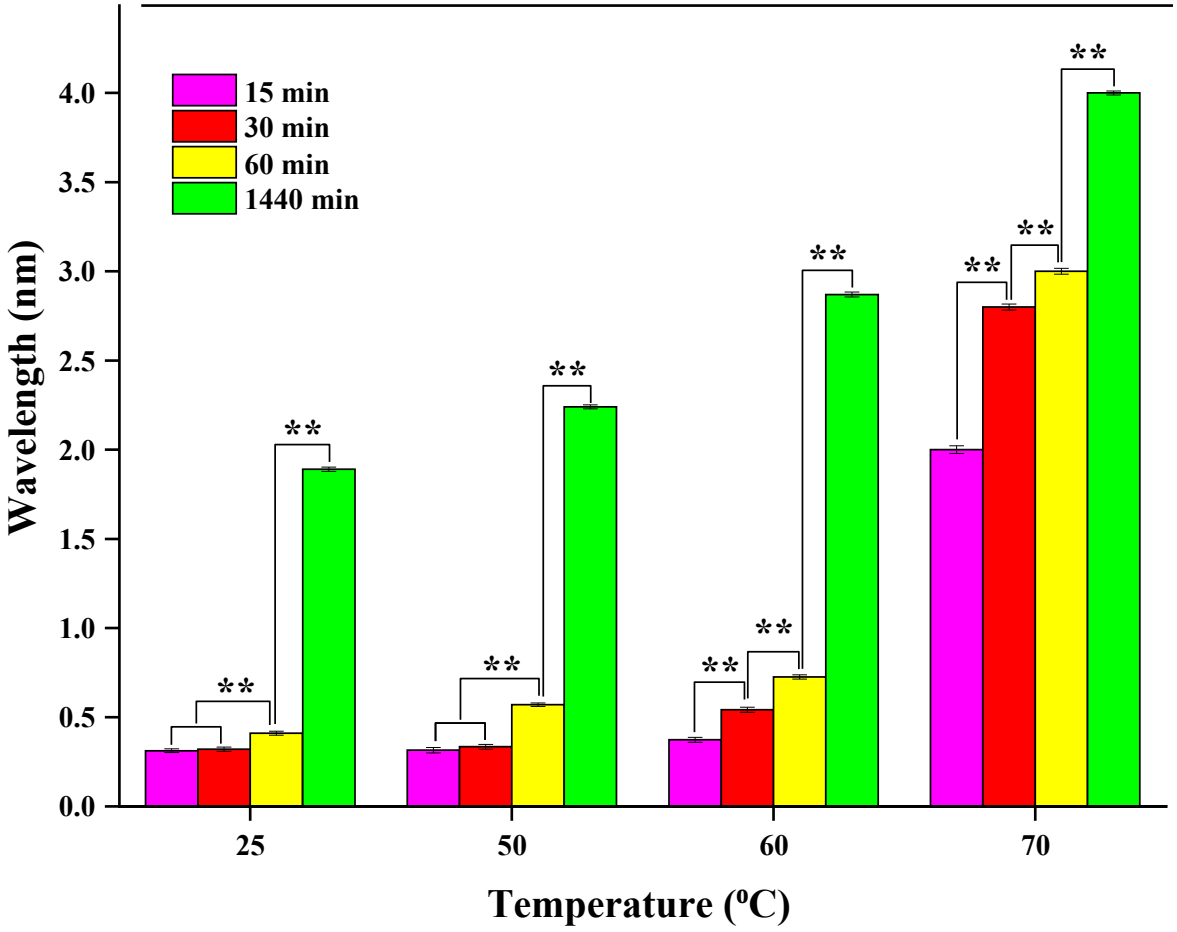

Fig. 3 Effect of temperature on the synthesis of AgNPs. The graph shows the variation in nanoparticle formation at different temperatures. Indicates statistically significant differences between groups ($P < 0.05$).

3.3. Characterization Techniques for the Synthesized Silver Nanoparticles

3.3.1. UV-Vis spectral analysis

UV–Vis spectroscopy recorded over the wavelength range of 220–620 nm, which showed a clear surface plasmon resonance (SPR) band, confirmed the synthesis of AgNPs [34]. This noticeable absorption peak is caused by the collective oscillations of conduction electrons on the surface of the nanoparticle when they are excited by incoming light; this phenomenon is known as localized surface plasmon resonance (LSPR) [35]. The prominent and distinct SPR peak at $\lambda max \approx 420$ nm, shown in **Fig. 4**, verifies the successful synthesis of AgNPs with a reasonably consistent

particle size distribution [36]. Furthermore, this peak is a reliable indicator of nanoparticle formation and stability because its position, intensity, and shape are influenced by variables such as particle size, morphology, concentration, and the surrounding environment, consistent with previously reported AgNP studies [37].

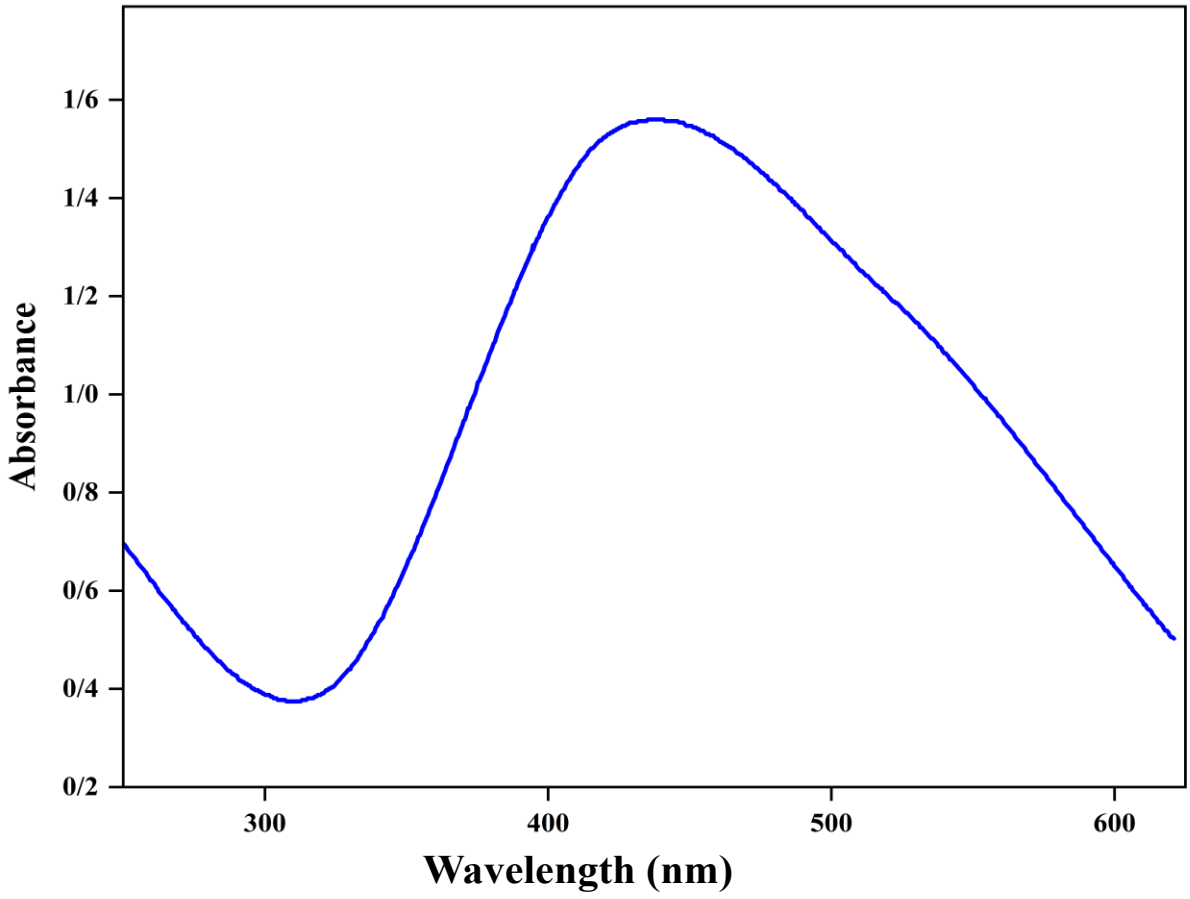

Fig. 4 UV–Vis spectrum of AgNPs synthesised using *M. spicata* extract over the wavelength range 220–620 nm.; the prominent and distinct SPR peak at λmax ≈ 420 nm

3.3.2. FTIR analysis

The FTIR spectra of *M. spicata* extract combined with $AgNO_3$ were recorded over the 400–4000 cm^{-1} range, as shown in **Fig. 5-a**. The spectra indicate the presence of several functional groups and phytochemical constituents that may participate in the biosynthesis of silver nanoparticles. Phytochemical examination of the extract in the presence of $AgNO_3$ suggested the coexistence of bioactive compounds, including phenolic and flavonoid-related functional groups, which are commonly reported to be involved in nanoparticle formation [38, 39]. The spectrum therefore

reflects the interaction between Ag^+ ions and plant-derived biomolecules, rather than confirming specific molecular identities [40].

The FTIR spectra presented in **Fig. 5-b** compare the synthesized AgNPs with the ethanolic extract of *M. spicata* leaves. A broad absorption band around 3423 cm^{-1} observed in the leaf extract is attributed to the stretching vibrations of hydroxyl (-OH) groups, commonly found in alcohols and phenols [41]. A shift from 2977 cm^{-1} to 2898 cm^{-1} was noted, corresponding to C–H stretching vibrations typical of aliphatic compounds [42]. The peak at 1647 cm^{-1} is associated with carbonyl (C=O) stretching vibrations, whereas the band at 1047 cm^{-1} relates to C–O functional groups [18]. Furthermore, the signal near 1452 cm^{-1} may be attributed to C–N stretching vibrations in aliphatic amines[18,38, 41].

In the spectrum of the synthesized AgNPs, the -OH absorption shifted slightly to 3427 cm^{-1}, and C–H stretching bands moved from 2856 cm^{-1} to 2925 cm^{-1} [24]. Peaks observed in the 1173–1262 cm^{-1} region are commonly assigned to C–O stretching vibrations, which are frequently reported in polyphenolic and flavonoid-containing compounds, while the carbonyl-related absorption appeared in the range of 1606–1724 cm^{-1} [43]. The band detected at approximately 1458 cm^{-1} can be associated with C–N stretching vibrations of aliphatic amine groups [18, 41].

Comparison of the two spectra reveals noticeable shifts in several absorption bands, indicating possible interactions between silver ions and plant-derived functional groups during nanoparticle formation [44]. The shift in –OH stretching frequency from 3423 to 3427 cm^{-1} suggests the involvement of hydroxyl-containing compounds, such as phenolics and alcohols, in the reduction and stabilization processes [24].

Overall, the FTIR results suggest that polyphenolic compounds, including flavonoids present in *M. spicata*, may contribute to the reduction and capping of silver nanoparticles. However, FTIR analysis alone does not allow definitive identification of the specific phytochemicals involved, and the proposed roles are based on functional group interactions commonly reported in plant-mediated nanoparticle synthesis [24].

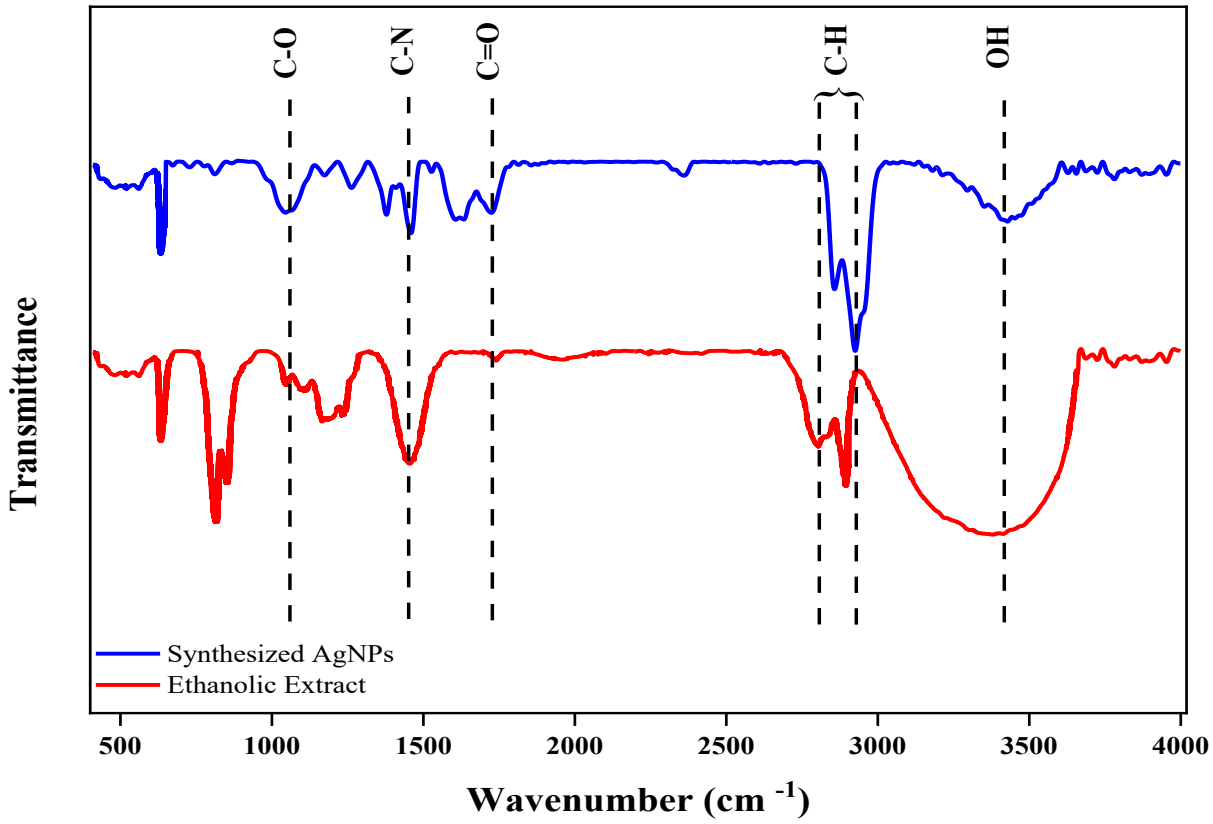

Fig. 5 (a-Red) FTIR spectra of an ethanolic extract of the *M. spicata*; (b-Blue) FTIR image of synthesized AgNPs

3.3.3. XRD analysis

X-ray diffraction (XRD) analysis was used to examine the crystal structure of AgNPs made with *M. spicata* extract [24]. The diffraction pattern displayed in Fig. 6 shows prominent peaks at 2θ = 37.95°, 44.45°, 64.45°, and 77.35°, corresponding to the (111), (200), (220), and (311) planes of face-centered cubic (fcc) metallic silver [24]. The appearance of these characteristic peaks confirms that crystalline AgNPs were successfully synthesized, as the diffraction angles match those listed in the standard JCPDS file (card no. 04-0783).

The average crystallite size (D) of the AgNPs was calculated using the Scherrer equation applied to the (111) peak, resulting in D ≈ 13 nm. This value represents the size of the crystalline core of the nanoparticles.

Furthermore, the sharpness and intensity of the diffraction peaks reflect the high crystallinity of the synthesized AgNPs, supporting their uniform formation and structural stability [45].

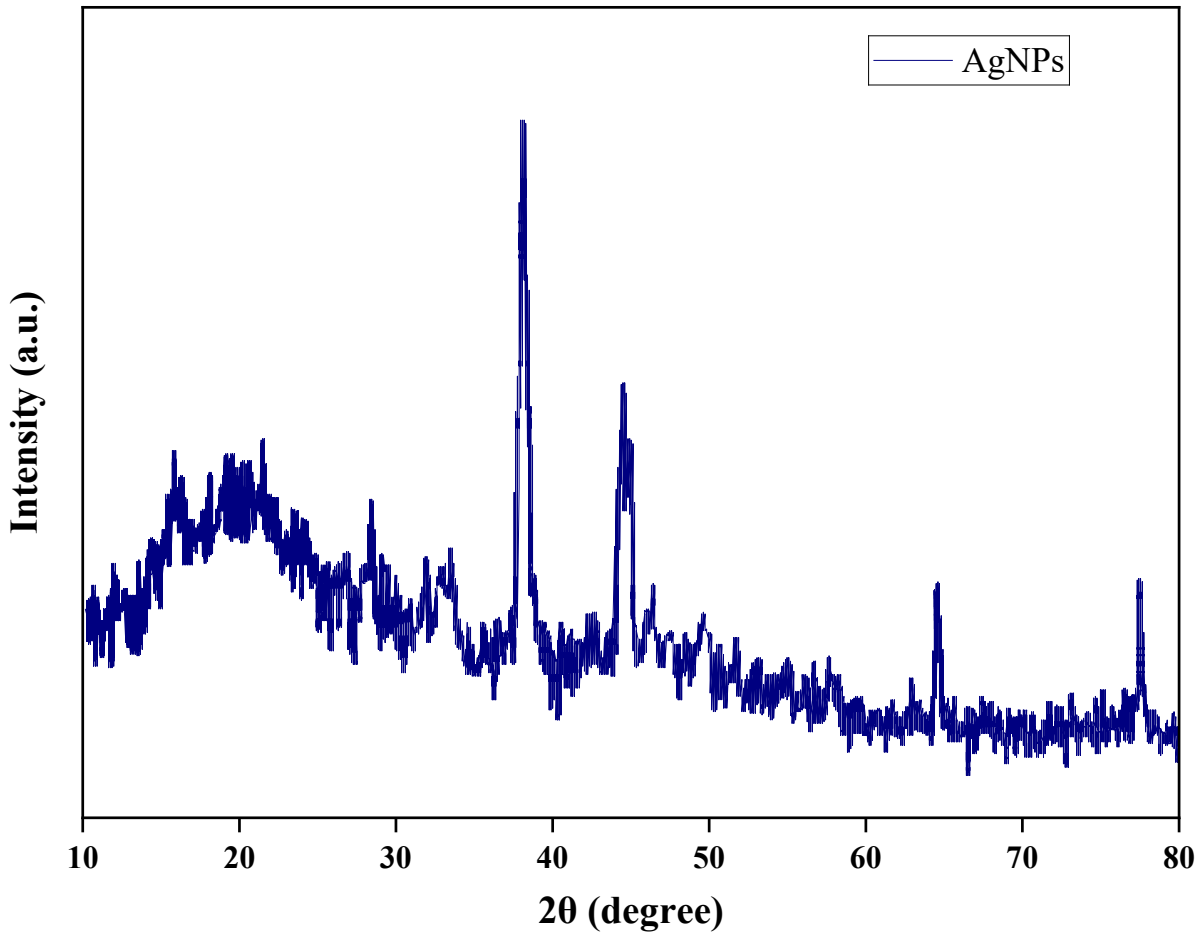

Fig. 6 XRD pattern of AgNPs

3.3.4. SEM analysis

Using scanning electron microscopy, the biosynthesized silver nanoparticles' morphology and dimensional properties were investigated [24]. This method uses a concentrated electron beam to create high-resolution, detailed images of the sample surface that enable precise observation of the size distribution and shape of the particles [46]. SEM micrographs of AgNPs synthesized under optimized conditions are shown in **Fig. 7**. Analysis of the images indicates that the majority of nanoparticles exhibit a roughly spherical shape with an average diameter of approximately 58.41 nm [41]. This measured size is larger than the crystallite size obtained from XRD (~13 nm), which represents only the crystalline core of the nanoparticles. The difference reflects the presence of a stabilizing layer and any aggregation of particles, while the consistency in size and shape observed across the sample confirms that the green synthesis method produces nanoparticles with uniform morphology.

Overall, the combination of XRD and SEM results provides complementary information: XRD confirms the crystalline nature and core size, while SEM demonstrates the overall particle size, shape, and uniformity, addressing concerns regarding nanoparticle characterization and reproducibility [47].

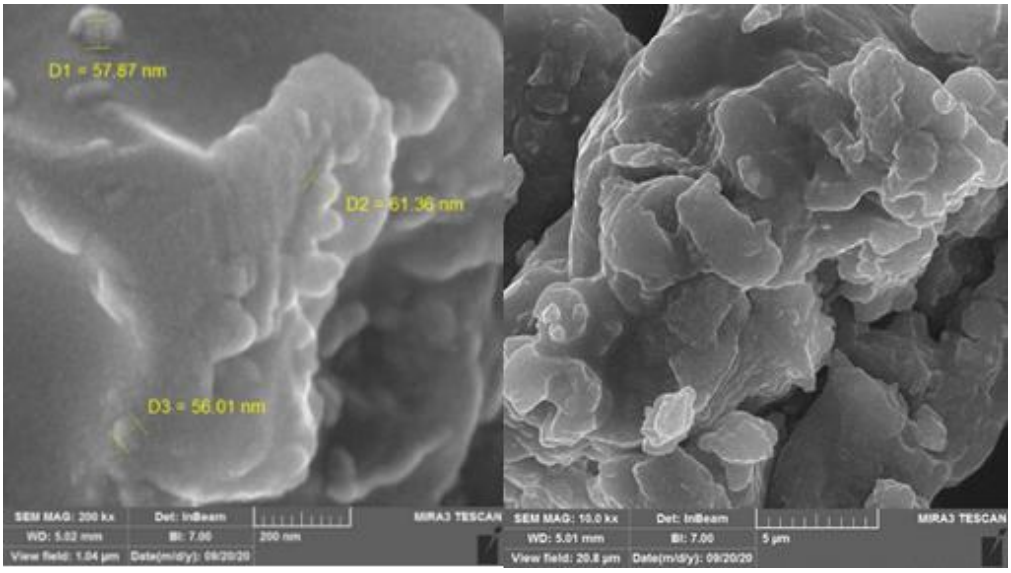

Fig. 7 Scanning Electron Microscopy of biosynthesized silver nanoparticles' morphology and dimensional properties, showing a rough spherical shape with an average diameter of approximately 58.41 nm (diameters D -D1=57.87, D2=61.36, D3= 56.01, shown in yellow font over particles in micrograph)

3.3.5. Antioxidant activity of the *M. spicata* plant

Antioxidant activity of the *M. spicata* plant The Folin–Ciocalteu method was used to measure the total phenolic content of the *M. spicata* ethanolic extract used in the synthesis of silver nanoparticles. The result was 106.22 mg gallic acid equivalents (GAE) per gram of dried plant material [48]. The DPPH assay 51 was used to measure the extract's antioxidant capacity by looking at how well it neutralized free radicals [49]. In comparison to the standard antioxidant, vitamin C, which demonstrated an IC50 value of 8.86 µg/mL, the concentration needed to achieve 50% radical inhibition (IC50) for the *M. spicata* extract was found to be 34.0217 µg/mL, indicating a moderate antioxidant potential [50]. The inhibition curve showing the extract's antioxidant activity is shown in **Fig. 8** [49]. These results demonstrate that *M. spicata* exhibits significant free radical scavenging capacity, with a lower IC50 value corresponding to stronger antioxidant activity [48].

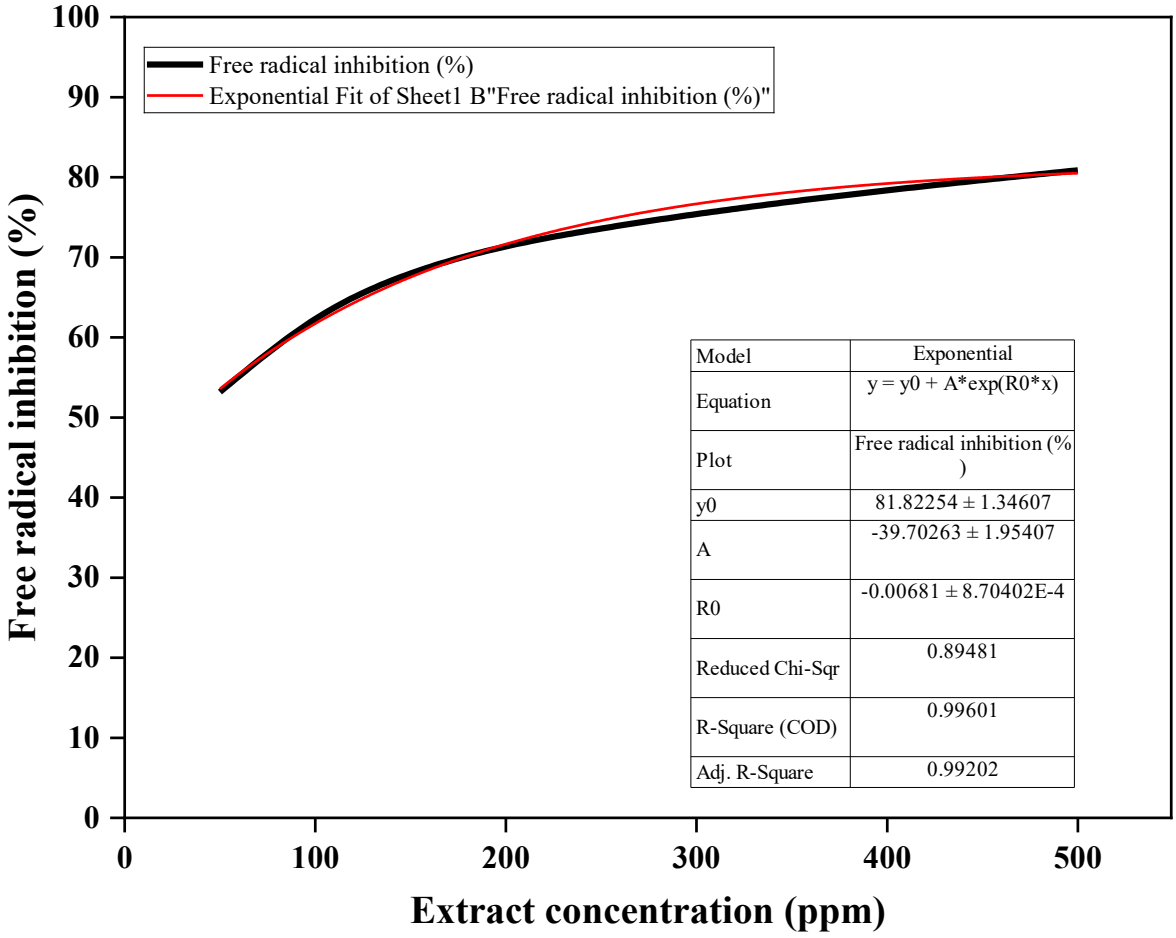

Fig. 8 Inhibition of free radicals by *M. spicata* extract

3.4. Antibacterial Activity of Synthesised Nanoparticles

3.4.1. Disc Diffusion Method

AgNPs synthesised using *M. spicata* leaf extract exhibited significant antibacterial activity, particularly at higher concentrations [24. 51]. The inhibitory effect of AgNPs on bacterial growth was concentration-dependent [51, 52]. As the concentration of the AgNPs solution decreased, the bacterial resistance to inhibition increased correspondingly [53]. **Fig. 9** illustrates the antibacterial effect, comparing the inhibition zones produced by the synthesised AgNPs (panel A) with those produced by standard antibiotic controls (panel B) against the tested bacterial strains. The presence of clear zones surrounding the discs demonstrates the strong antibacterial activity exhibited by the AgNPs biosynthesised from *M. spicata* [17, 54].

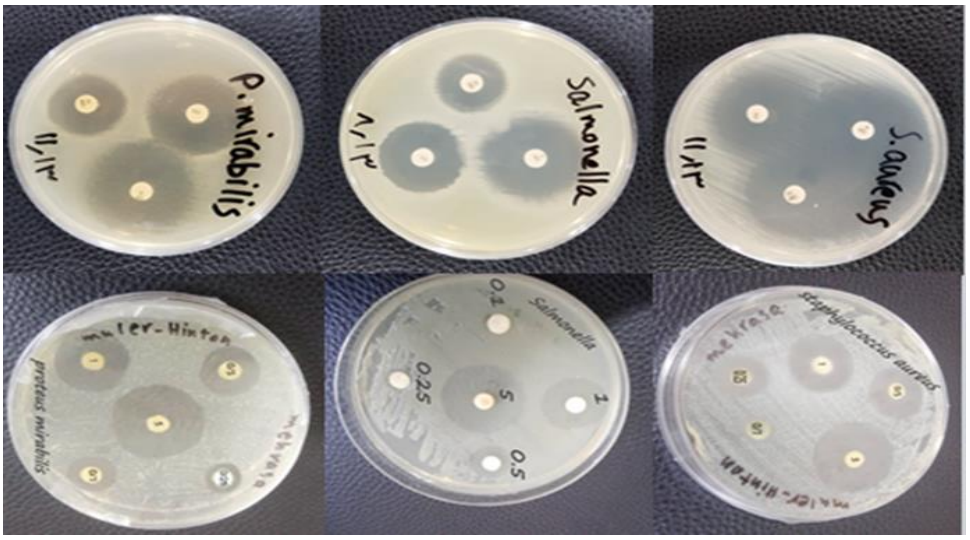

Fig. 9 The diameter of inhibition zone of bacterial growth caused by synthesised AgNPs(A) and control antibiotics (B) on the tested bacteria

3.4.2. Tube Dilution Method

To evaluate microbial growth inhibition, the optimal extract obtained via ultrasonication was tested. **Table 3**, presents the inhibitory effects of AgNPs at concentrations of 5, 1, 0.5, 0.25, and 0.1 mg/mL, as well as demonstrating a clear dose-dependent response comparable to standard antibiotics. The AgNPs showed their highest antibacterial potency against *S. aureus*, while their effectiveness was least pronounced against *S. typhimurium* [54]. The data indicate that while the *M. spicata* plant extract alone showed no significant antibacterial activity against the tested bacterial strains, the AgNPs synthesized from the extract effectively inhibited bacterial growth [51, 55, 56]. The preliminary screening using the tube dilution method was performed to identify the effective concentration range of the synthesized AgNPs. Based on these observations, a concentration gradient of 0.1 to 5 mg/mL was selected for the detailed Disc Diffusion assay. The results of the tube dilution were consistent with the inhibition zones reported in Table 2, confirming the dose-dependent antibacterial activity.

Table 3. Diameter of inhibition zones (mm) caused by different concentrations of AgNPs synthesised from *M. spicata* extract and by control antibiotics against tested Gram-positive and Gram-negative bacteria

Bacterial Strains	**Zone of Inhibition (mm)**							
	Concentration (mg/mL)					**Standard Control Antibiotics**		
	5	**1**	**0.5**	**0.25**	**1**	**Ciprofloxacin**	**Gentamicin**	**Sulfamethoxazole trimethoprim**
S. aureus ATCC29212	14 ± 0.2 [a]	11 ± 0.1 [a]	9 ± 0.1 [b]	8 ± 0.1 [a]	6 ± 0.1 [a]	15 ± 0.3 [b]	15 ± 0.4 [a]	12 ± 0.2 [a]
Proteus mirabilis	13 ± 0.1 [b]	11 ± 0.2 [a]	9.3 ± 0.1 [a]	7.5 ± 0.2 [b]	3 ± 0.1 [b]	16 ± 0.4 [a]	9 ± 0.3 [b]	6 ± 0.1 [b]
S. typhimurium ATCC14028	12 ± 0.2 [c]	9 ± 0.2 [b]	7 ± 0.1 [c]	0 [c]	0 [c]	8 ± 0.1 [c]	7 ± 0.1 [c]	5 ± 0.1 [c]

Results are expressed as mean ± standard deviation (SD) (n = 3). Statistical analysis was performed using one-way analysis of variance (ANOVA) followed by Tukey's post hoc test in SPSS software. Differences were considered statistically significant at $p < 0.05$. Mean values in the same column with different superscript letters (a–c) indicate significant differences.

4. Conclusion

Our studies have shown that *M. spicata,* a native plant of Mazandaran province, is a rich source of polyphenols. Its phenolic compounds have shown to have antioxidant qualities and biological activities of medicinal advantages. This study was useful in comparing a number of methods of extraction, including Soxhlet, maceration, and ultrasonic extraction. At a solid-to-solvent ratio of 1:20 (g/ml), ultrasonic extraction showed the best efficiency. The IC50 value of the ultrasonic extraction extract was 34.0217 µg/mL. Additionally, there were 106.22 mg of gallic acid per gram in the dried plant material. A color shift from colorless to brown signified the synthesis of AgNPs. The ideal conditions for synthesis were established at pH 9.0, 60 °C, and 1 g/L extract concentration after a number of variables, including temperature, pH level, extract concentration, and reaction time, were optimised. XRD confirmed the structural properties of AgNPs. The phenolic compounds in *M. spicata* extract were crucial in lowering silver ions and stabilizing the nanoparticles, according to FTIR analysis. as confirmed in SEM analysis, the particles of 58.41 nm size can be successfully prepared. As our results have proved that AgNPs can be used to reduce the growth of Gram positive and negative bacterial strains.

5. Future work

Antibacterial and antioxidant qualities make nanoparticles, synthesised from plant resources, extremely promising for a range of applications. For future work, we plan to prepare nanoparticles using natural, common edible material [57-60] and medicinal plant roots, including *Rubia cordifolia* [61], *Withania somnifera* [62], which have been identified in research studies as being rich in antibiotic and antioxidant activities [57-63]. Nanoparticles prepared from such renewable resources can be used as antimicrobial agents in pharmaceutical formulations, wound dressings to promote healing and prevent infections, as well as prepared from edible resources, these can be used for innovative packaging materials for short shelf-life expensive food products [64, 65]. Furthermore, their biocompatibility and environmentally friendly synthesis process point to potential applications in targeted drug delivery systems, biomedical devices, and cosmetics. Additionally, the nanoparticles may be investigated for use as catalysts in chemical reactions and in environmental applications like water purification. Such applications would be contributing to the economy in achieving Sustainable Development Goals.

List of Abbreviations

TPC	Total phenolic content
M. spicata	*Mentha spicata*
IC_{50} (IC50)	Half-maximal inhibitory concentration
FTIR	Fourier-transform infrared spectroscopy

GAE	Gallic acid equivalents
DPPH	2,2-Diphenyl-1-picrylhydrazyl
ATCC	American Type Culture Collection
DMSO	Dimethyl sulfoxide
SD	Standard deviation
SEM	Scanning electron microscopy
AgNPs	Silver Nanoparticles
XRD	X-ray diffraction
P. mirabilis	*Proteus mirabilis*
S. typhimurium	*Salmonella typhimurium*
S. aureus	*Staphylococcus aureus*

Author Contributions: S Mousavi and P Ashooriyan: investigation, software, methodology, formal analysis, validation, writing original draft; S Mousavi, P Ashooriyan, M Y Rostami and M Erfani: investigation, methodology, formal analysis, validation, writing original draft, writing review and editing; PS Nigam: supervision, writing, review and editing; S Mousavi, P Ashooriyan, MY Rostami, and M Erfani: visualization, funding acquisition. All authors have read and agreed to the published version of the manuscript.

Availability of data and materials: All data included in this study are available upon request.

Conflicts of Interest: The authors declare no conflicts of interest.

Funding

This research funding was granted to the Department of Biotechnology at the Faculty of Chemical Engineering by the Babol Noshirvani University of Technology, for research work conducted by S Mousavi, P Ashooriyan, MY Rostami, and M Erfani.

Acknowledgements: The authors extend their appreciation to Babol Noshirvani University of Technology, Faculty of Chemical Engineering, for providing financial support for this project. The authors sincerely thank Dr Morteza Hossieni (Department of Chemical Engineering; Babol Noshirvani University of Technology) for his valuable guidance throughout this research.

AI-declaration

The authors acknowledge the use of ChatGPT (OpenAI) solely for language editing and grammatical improvement of manuscript. The scientific content, data analysis, and interpretation of results were entirely conducted by the authors and they take full responsibility for the accuracy and integrity of the work.

References

1. Alavi M, Kamarasu P, McClements DJ, et al. Metal and metal oxide-based antiviral nanoparticles: Properties, mechanisms of action, and applications. Advances in Colloid and Interface Science 2022;306(102726, doi:https://doi.org/10.1016/j.cis.2022.102726
2. Tanwar SN, Parauha YR, There Y, et al. Plant-Based Biosynthesis of Metal and Metal Oxide Nanoparticles: An Update on Antimicrobial and Anticancer Activity. ChemBioEng Reviews 2024;11(6):e202400012, doi:https://doi.org/10.1002/cben.202400012
3. Panwar MS, Pal P, Joshi D. Advances in Green Synthesis of Silver Nanoparticles: Sustainable Approaches and Applications. Journal of Drug Delivery & Therapeutics 2024;14(11), doi:https://doi.org/10.22270/jddt.v14i11.6854
4. Jeevanandam J, Kiew SF, Boakye-Ansah S, et al. Green approaches for the synthesis of metal and metal oxide nanoparticles using microbial and plant extracts. Nanoscale 2022;14(7):2534–2571, doi:https://doi.org/10.1039/D1NR08144F
5. Adelere IA, Lateef A. A novel approach to the green synthesis of metallic nanoparticles: the use of agro-wastes, enzymes, and pigments. Nanotechnology Reviews 2016;5(6):567–587, doi:https://doi.org/10.1515/ntrev-2016-0024
6. Hussain AI, Anwar F, Chatha SAS, Jabbar A, et al. *Rosmarinus officinalis* essential oil: antiproliferative, antioxidant and antibacterial activities. *Brazilian J. of Microbiology* 2010; 41 (4), 1070-1078.
7. Hussain AI, Anwar F, Nigam P, Ashraf M, Gilani AH. Seasonal Variation in Content, Chemical Composition and Antimicrobial and Cytotoxic Activities of Essential Oils from Four Mentha Species. *J. of Science of Food and Agriculture*, 2010; 90, 1827-1836.
8. Silva BN, Cadavez V, Caleja C, et al. Phytochemical composition and bioactive potential of Melissa officinalis L., Salvia officinalis L. and Mentha spicata L. extracts. Foods 2023;12(5):947, doi:https://doi.org/10.3390/foods12050947
9. Nouri A, Yaraki MT, Lajevardi A, et al. Ultrasonic-assisted green synthesis of silver nanoparticles using Mentha aquatica leaf extract for enhanced antibacterial properties and catalytic activity. Colloid and Interface Science Communications 2020;35(100252, doi:https://doi.org/10.1016/j.colcom.2020.100252
10. Ojewumi ME, Adedokun SO, Ayoola AA, et al. Evaluation of the oil Extract from Mentha spicata and its Chemical Constituents. International Journal of Sciences and Research 2018;74(11/1), doi:http://dx.doi.org/10.21506/j.ponte.2018.11.7
11. Thantry ADK, Chakravarthi KK, Thundakattil AV, et al. Traditional Aqueous and Ethanol Maceration of Hamelia patens Leaves: A Phytochemical and Pharmacological Exploration. Annals of African Medicine 2025;10.4103, doi:https://doi.org/10.4103/aam.aam_152_25
12. Vanlalveni C, Lallianrawna S, Biswas A, et al. Green synthesis of silver nanoparticles using plant extracts and their antimicrobial activities: A review of recent literature. RSC advances 2021;11(5):2804–2837, doi:https://doi.org/10.1039/D0RA09941D
13. Qaeed MA. Examining the varied concentrations of Mentha spicata and Ocimum basilicum affect the synthesis of AgNPs that restrict the development of bacteria. Saudi Journal of Biological Sciences 2024;31(1):103899, doi:https://doi.org/10.1016/j.sjbs.2023.103899

14. Badawy AME, Luxton TP, Silva RG, et al. Impact of environmental conditions (pH, ionic strength, and electrolyte type) on the surface charge and aggregation of silver nanoparticles suspensions. Environmental science & technology 2010;44(4):1260–1266, doi:https://doi.org/10.1021/es902240k
15. Ansari M, Ahmed S, Abbasi A, et al. Plant mediated fabrication of silver nanoparticles, process optimization, and impact on tomato plant. Scientific Reports 2023;13(1):18048, doi:https://doi.org/10.1038/s41598-023-45038-x
16. Farooq U, Qureshi AK, Noor H, et al. Plant extract-based fabrication of silver nanoparticles and their effective role in antibacterial, anticancer, and water treatment applications. Plants 2023;12(12):2337, doi:https://doi.org/10.3390/plants12122337
17. Torres-Martínez Y, Arredondo-Espinoza E, Puente C, et al. Synthesis of silver nanoparticles using a Mentha spicata extract and evaluation of its anticancer and cytotoxic activity. PeerJ 2019;7(e8142, doi:https://doi.org/10.7717/peerj.8142/fig-3
18. Umar H, Aliyu MR, Ozsahin DU. Iron oxide nanoparticles synthesized using Mentha spicata extract and evaluation of its antibacterial, cytotoxicity and antimigratory potential on highly metastatic human breast cells. Biomedical Physics & Engineering Express 2024;10(3):035019, doi:https://doi.org/10.1088/2057-1976/ad3646
19. Ramzan M, Abusalah MAHA, Ahmed N, et al. Green Synthesis and Characterization of Silver Nanoparticles Using Zingiber officinale Extracts to Investigate Their Antibacterial Potential. International Journal of Nanomedicine 2024;13319–13338, doi:https://doi.org/10.2147/IJN.S475656
20. Annamalai J, Nallamuthu T. Green synthesis of silver nanoparticles: characterization and determination of antibacterial potency. Applied nanoscience 2016;6(2):259–265, doi:https://doi.org/10.1007/s13204-015-0426-6
21. Ashooriyan P, Mohammadi M, Darzi GN, et al. Development of Plantago ovata seed mucilage and xanthan gum-based edible coating with prominent optical and barrier properties. International Journal of Biological Macromolecules 2023;248(125938, doi:https://doi.org/10.1016/j.ijbiomac.2023.125938
22. Hudzicki J. Kirby-Bauer disk diffusion susceptibility test protocol. American society for microbiology 2009;15(1):1–23
23. Qaeed MA, Hendi A, Thahe AA, et al. Effect of different ratios of mentha spicata aqueous solution based on a biosolvent on the synthesis of agnps for inhibiting bacteria. Journal of Nanomaterials 2023;2023(1):3599501, doi:https://doi.org/10.1155/2023/3599501
24. Moosavy M-H, de la Guardia M, Mokhtarzadeh A, et al. Green synthesis, characterization, and biological evaluation of gold and silver nanoparticles using Mentha spicata essential oil. Scientific Reports 2023;13(1):7230
25. Calubaquib MAM, Delfin EF, Merca FE, et al. Biogenic synthesis and characterization of silver nanoparticles (AgNPs) produced by indigenous microorganisms isolated from banana (Musa spp) soils. 2023, doi:http://dx.doi.org/10.18006/2023.11(1).105.118
26. Flieger J, Franus W, Panek R, et al. Green synthesis of silver nanoparticles using natural extracts with proven antioxidant activity. Molecules 2021;26(16):4986, doi:https://doi.org/10.3390/molecules26164986
27. Ghosh S, Patil S, Ahire M, et al. Synthesis of silver nanoparticles using Dioscorea bulbifera tuber extract and evaluation of its synergistic potential in combination with antimicrobial agents. International journal of nanomedicine 2012;483–496, doi:https://doi.org/10.2147/IJN.S24793
28. Amaladhas TP, Sivagami S, Devi TA, et al. Biogenic synthesis of silver nanoparticles by leaf extract of Cassia angustifolia. Advances in Natural Sciences: Nanoscience and Nanotechnology 2012;3(4):045006, doi:https://doi.org/10.1088/2043-6262/3/4/045006
29. Miranda A, Akpobolokemi T, Chung E, et al. pH alteration in plant-mediated green synthesis and its resultant impact on antimicrobial properties of silver nanoparticles (AgNPs). Antibiotics 2022;11(11):1592, doi:https://doi.org/10.3390/antibiotics11111592

30. Kamarudin D, Hashim NA, Ong BH, et al. Synthesis of silver nanoparticles stabilised by pvp for polymeric membrane application: a comparative study. Materials Technology 2022;37(5):289–301
31. Razali Z, Norrizah J, Abdullah S. Impact of temperature and pH on antioxidant activity of green silver nanoparticles fabricated from Ananas comosus peel extracts. IOP Publishing: 2022.
32. Liu H, Zhang H, Wang J, et al. Effect of temperature on the size of biosynthesized silver nanoparticle: Deep insight into microscopic kinetics analysis. Arabian Journal of Chemistry 2020;13(1):1011–1019, doi:https://doi.org/10.1016/j.arabjc.2017.09.004
33. Kaur R, Avti P, Kumar V, et al. Effect of various synthesis parameters on the stability of size controlled green synthesis of silver nanoparticles. Nano Express 2021;2(2):020005, doi:https://doi.org/10.1088/2632-959X/abf42a
34. Ibrahim NH, Taha GM, Hagaggi NSA, et al. Green synthesis of silver nanoparticles and its environmental sensor ability to some heavy metals. BMC chemistry 2024;18(1):7, doi:https://doi.org/10.1186/s13065-023-01105-y
35. Cao W, Huang T, Xu X-HN, et al. Localized surface plasmon resonance of single silver nanoparticles studied by dark-field optical microscopy and spectroscopy. Journal of applied physics 2011;109(3), doi:https://doi.org/10.1063/1.3544349
36. Paul TK, Jalil MA, Pranto Kumar Mondal MM, et al. Morphological Characterization of Bio-Mediated Silver Nanoparticles from Azadirachta Indica (Neem) Leaf Extract. 2022.
37. Zhan Z, Xu R, Mi Y, et al. Highly controllable surface plasmon resonance property by heights of ordered nanoparticle arrays fabricated via a nonlithographic route. ACS nano 2015;9(4):4583–4590, doi:https://doi.org/10.1021/acsnano.5b01226
38. Chatterjee A, Singh N, Chanu WK, et al. Phytochemical screening, cytotoxicity assessment and evaluation of in vitro antiplasmodial and in vivo antimalarial activities of Mentha spicata L. methanolic leaf extract. Journal of ethnopharmacology 2022;298(115636, doi:https://doi.org/10.1016/j.jep.2022.115636
39. El Menyiy N, Mrabti HN, El Omari N, et al. Medicinal uses, phytochemistry, pharmacology, and toxicology of Mentha spicata. Evidence-Based Complementary and Alternative Medicine 2022;2022(1):7990508, doi:https://doi.org/10.1155/2022/7990508
40. Gwada CA, Ndivhuwo PS, Matshetshe K, et al. Phytochemical-assisted synthesis, optimization, and characterization of silver nanoparticles for antimicrobial activity. RSC advances 2025;15(18):14170–14181, doi:https://doi.org/10.1039/D4RA08900F
41. Khalid Z, Javed A, Alyas T, et al. Biosynthesis, structural characterization of silver nanoparticles synthesized using an eco-friendly method with Mentha spicata L. extract and their antimicrobial activity and toxicological risk assessment. Results in Chemistry 2024;7(101487, doi:https://doi.org/10.1016/j.rechem.2024.101487
42. Mat Yusuf SNA, Che Mood CNA, Ahmad NH, et al. Optimization of biogenic synthesis of silver nanoparticles from flavonoid-rich Clinacanthus nutans leaf and stem aqueous extracts. Royal Society open science 2020;7(7):200065
43. Al-Zahrani S, Astudillo-Calderón S, Pintos B, et al. Role of synthetic plant extracts on the production of silver-derived nanoparticles. Plants 2021;10(8):1671
44. Mustapha T, Misni N, Ithnin NR, et al. A review on plants and microorganisms mediated synthesis of silver nanoparticles, role of plants metabolites and applications. International Journal of Environmental Research and Public Health 2022;19(2):674, doi:https://doi.org/10.3390/ijerph19020674
45. Ali MH, Azad MAK, Khan K, et al. Analysis of crystallographic structures and properties of silver nanoparticles synthesized using PKL extract and nanoscale characterization techniques. ACS omega 2023;8(31):28133–28142, doi:https://doi.org/10.1021/acsomega.3c01261
46. Erdman N, Bell DC, Reichelt R. Scanning Electron Microscopy. In: Springer Handbook of Microscopy. (Hawkes PW, Spence JCH. eds.) Springer International Publishing: Cham; 2019; pp. 229–318.

47. Nagilla B, Ajmeera A, Sultana K, et al. The Synthesis and Characterization of Mint Leaf (Mentha Spicata) Biological Silver Nanoparticles and their Impact on Rat's Motor Coordination and Cognition. International Journal of Pharmaceutical Sciences and Nanotechnology (IJPSN) 2024;17(6), doi:https://doi.org/10.37285/ijpsn.2024.17.6.3
48. Kaddour A, Amara DG, Moussaoui Y, et al. Total phenolic and flavonoid contents of Mentha spicata leaves aqueous extracts in different regions of Algeria and their antioxidant, and antidiabetic activities. Tropical Journal of Pharmaceutical Research 2022;21(9):1907–1913, doi:https://doi.org/10.4314/tjpr.v21i9.14
49. Brahmi F, Nury T, Debbabi M, et al. Evaluation of antioxidant, anti-inflammatory and cytoprotective properties of ethanolic mint extracts from algeria on 7-ketocholesterol-treated murine RAW 264.7 macrophages. Antioxidants 2018;7(12):184, doi:https://doi.org/10.3390/antiox7120184
50. Jamous RM, Abu-Zaitoun SY, Akkawi RJ, et al. Anti-obesity and antioxidant potentials of selected Palestinian medicinal plants. Evidence-Based Complementary and Alternative Medicine 2018;2018(1):8426752, doi:https://doi.org/10.1155/2018/8426752
51. Khan H, Andleeb S, Nisar T, et al. Interactions of Chitosan-coated Green Synthesized Silver Nanoparticles using Mentha spicata and Standard Antibiotics against Bacterial Pathogens. Current Pharmaceutical Biotechnology 2023;24(2):203–212, doi:https://doi.org/10.2174/1389201023666220405120914
52. More PR, Pandit S, Filippis AD, et al. Silver nanoparticles: bactericidal and mechanistic approach against drug-resistant pathogens. Microorganisms 2023;11(2):369, doi:https://doi.org/10.3390/microorganisms11020369
53. Hashim N, Bashi AM, Jasim A. Biosynthesis of silver nanoparticles by mentha spicata ethanolic leaves extract and investigation the antibacterial activity. AIP Publishing LLC: 2019.
54. Abdullateef A, Unegbu IA, Halilu EM. Green synthesis of silver nanoparticles from Mentha spicata L. aqueous extract and evaluation of its antioxidant, antibacterial and anticancer activities. 2023, doi:https://doi.org/10.21203/rs.3.rs-3510631/v1
55. Abalaka ME, Akpor OB, Osemwegie OO. Green synthesis and antibacterial activities of silver nanoparticles against Escherichia coli, Salmonella typhi, Pseudomonas aeruginosa and Staphylococcus aureus. Advancements in Life Sciences 2017;4(2):60–65
56. Todorova M, Petrova V, Ranguelov B, et al. Green Synthesis of Antimicrobial Silver Nanoparticles (AgNPs) from the Mucus of the Garden Snail Cornu aspersum. Molecules 2025;30(10):2150, doi:https://doi.org/10.3390/molecules30102150
57. Bontzolis C, Plioni I, Dimitrellou D, Boura K, Kanellaki M, et al. Isolation of antimicrobial compounds from aniseed and techno-economic feasibility report for industrial-scale application. *International J of Food Science and Technology* 2022; 1-26. https://doi.org/10.1111/ijfs.15824.
58. Wan HC, Sultana B, Nigam P, Owusu-Apenten RK Comparison of Iron (III) Reducing Antioxidant Capacity (iRAC) and ABTS Radical Quenching Assays for Estimating Antioxidant Activity of Pomegranate. Beverages 2018; 4 (3), 1-10.
59. Chan YM, Cheng NK, Nigam P, Owusu-Apenten RK Effect of pH on the Radical Quenching Capacity of Tea Infusions Using the ABTS•+ Assay. *J. of Applied Life Sciences International* 2016; 6 (2), 1-8.
60. Cheung T, Nigam P, Owusu-Apenten RK Antioxidant Activity of Curcumin and Neem (*Azadirachta indica)* Powders: Combination Studies with ALA Using MCF-7 Breast Cancer Cells. *J. of Applied Life Sciences International* 2016; 4 (3), 1-12.
61. Barlow R, Barnes D, Campbell A, Owusu-Apenten R, et al. Antioxidant, Anticancer and Antimicrobial, Effects of *Rubia cordifolia* Aqueous Root Extract. *J. of Advances in Biology Biotechnology* 2015; 5 (1), 6-14.
62. Barnes, DA, Barlow R, Nigam P, Owusu-Apenten R Antioxidant, Anticancer and Antibacterial Activity of *Withania somnifera* Aqueous Root Extract. *J. of Advances in Biology Biotechnology* 2015; 5 (1), 1-6.

63. Efstratiou E, Hussain AI, Nigam P, et al. Antimicrobial Activity of *Callendula officinalis* petal extracts against fungi, as well as Gram-negative and Gram-positive clinical pathogens. *Complementary Therapies in Clinical Practice* 2012; 18 (3), 173-176.
64. Francis DV, Dahiya D, Kurup S, et al. Advancing Sustainability Through Circular Economy, Emerging Technologies and Bibliometric Insights Towards Innovative Biodegradable Packaging for Dairy Products, Contributing to Sustainable Development Goal 9, 12, 13.SCI Sustainability 2025; 1(1), e70005 https://doi.org/10.1002/sst2.70005.
65. Francis DV, Dahiya D, Gokhale T, et al. Sustainable packaging materials for fermented probiotic dairy or non-dairy food and beverage products: challenges and innovations. *AIMS Microbiology* 2024; 10(2): 320-339. www.doi.org/10.3934/microbiol.2024017